NATIONAL AERONAUTICS AND SPACE ADMINISTRATION

Technical Memorandum 33-794

Viking X-Band Telemetry Experiment Final Report

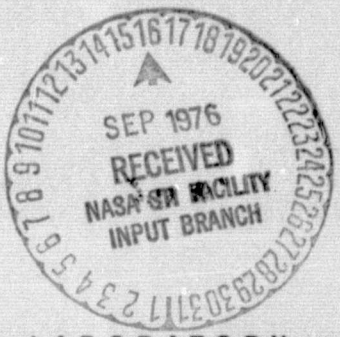

JET PROPULSION LABORATORY
CALIFORNIA INSTITUTE OF TECHNOLOGY
PASADENA, CALIFORNIA

September 1, 1976

PREFACE

The work described in this report was performed by the Telecommunications Division of the Jet Propulsion Laboratory.

ACKNOWLEDGMENT

The authors wish to thank the dozens of people in the DSN, the Viking Project, and Division 33 who contributed their time and effort in making this experiment a success. Special thanks to Ted Takahashi of Section 339 who recorded much of the data at DSS14, to Muriel Easterling of Section 339, who handled the computer reduction of the data, and to Robert Weber of Section 332 who wrote the required DSN engineering change orders and expedited their approval and implementation.

CONTENTS

FIGURES

ABSTRACT

In 1977 Mariner Jupiter-Saturn will be the first interplanetary spacecraft to use X-band frequencies for telemetry. In order to uncover operational and design problems in the use of X-band by MJS and future spacecraft using the Deep Space Network, an X-band telemetry experiment was conceived in 1973 and conducted in 1974 using the Mariner Venus-Mercury spacecraft. The Viking X-band telemetry experiment is a continuation of this earlier experiment with similar goals and expanded objectives.

The experiment was conducted at DSS-14 during the months of December 1975 and January 1976. During each of the five successful passes, a periodic sequence (in lieu of ranging) was transmitted to the spacecraft and returned by the spacecraft transponder on both S- and X-bands. These telemetry-like signals were received, demodulated, and detected. From a variety of measurements at the station, four independent measurements were made of the received signal-to-noise ratio (SNR). These four SNRs were later compared with each other and the predicted SNR.

The principal result of the experiment is that X-band telemetry works as expected. That is, the measured SNRs were consistent relative to each other and to the predicted values within the accuracy of the experiment. X-band performance as a function of weather was not obtained because of clear weather during each pass.

As a result of the need for weather performance data, the experimenters recommend the installation at one or more of the 64 meter stations the following: an accurate and complete weather data gathering facility including cloud observations; a noise adding radiometer for accurate X-band system noise temperature

recordings; and more accurate procedures and/or equipment for measuring X-band received carrier power. Data from this equipment in conjunction with normal Viking X-band signals could produce an extremely valuable performance baseline for MJS and future X-band missions.

I. INTRODUCTION

It is well known that for fixed antenna size and transmitter power that telemetry at X-band frequencies can outperform that at S-band frequencies by an order of magnitude in terms of signal-to-noise ratio. Because of this fact, the Mariner Jupiter-Saturn (MJS) Project has chosen X-band for its primary telemetry frequency band. While these frequencies have been used for years for a variety of uses, they have never been used for telemetry on an interplanetary spacecraft nor have such telemetry signals been received by the Deep Space Network (DSN). As a result of this lack of operational experience, an X-band telemetry experiment (XBTE)[1] was conceived in 1973 and made use of the transponder of the Mariner Venus-Mercury (MVM) spacecraft. The basic idea of the experiment was that a periodic sequence (in lieu of ranging) was transmitted to the spacecraft and returned by the transponder on both S- and X-bands. These received telemetry-like signals were then compared in terms of signal to noise ratio (SNR) and probability of error (P_E). It was hoped that, given sufficient spacecraft passes, this experiment could fill the gap of no operational X-band experience. Unfortunately, for a variety of reasons the MVM XBTE was successful for only a 70-minute pass.[1] The main conclusion of this experiment was that X-band telemetry did indeed appear to perform as expected. It was also concluded, however, that further tests were desirable to gain more knowledge and experience with this new telemetry mode. It was proposed at that time that a similar experiment be conducted with the Viking spacecraft.

The objectives of the Viking XBTE are virtually the same as the original MVM experiment. They are:

(1) To uncover and identify potential design or operational problems that may exist relative to the use of X-band

telemetry on future spacecraft missions so that early corrective measures can be taken.

(2) To gain a better knowledge of performance parameters and their tolerances.

(3) To quantitatively measure the performance of the X-band telemetry link to assess the effects of weather, elevation angle, coded burst-error statistics, etc.

(4) To test the proposed MJS convolutionally coded system at moderate and high (100 Kbps) data rates.

(5) To verify channel performance using SNRs typical of channel requirements for advanced coding methods proposed for compressed data transmission.

(6) To investigate and confirm the discrepancy from Gaussian behavior shown by the MVM XBTE.

It was felt that the key element needed for a successful experiment was a multitude of spacecraft passes. Variations in the weather were desirable which implied many passes to increase the chances for bad weather. As it turned out, the Viking Project did allow eleven passes to be used for the experiment during December 1975 and January 1976. Of these, five were successful passes in that for these five most of the desired measurements were made. Unfortunately, the longest dry spell in years occurred during this period so that essentially no weather variations were obtained. As described in the following sections, what was obtained was a fairly large amount of operational data which confirms that the X-band system does work as predicted.

II. EXPERIMENTAL TECHNIQUE

A. General Configuration

Figure 1 is a schematic diagram of the basic experimental technique. In lieu of ranging a subcarrier is modulated with a six bit periodic sequence as data. This signal is transmitted along with command modulation to the spacecraft. Because the subcarrier and its modulation appear in the ranging channel spectrum, it is retransmitted by the spacecraft S- and X-band transmitters. Thus, the downlink appears to have a subcarrier with telemetry data on both S- and X-bands. These telemetry channels are demodulated and detected. The detected outputs are then recorded and analyzed.

A more detailed description of the experiment is shown in Figure 2. All equipment shown in the control room is standard DSN equipment with the exception of the cable drivers. Wherever possible Block IV equipment was utilized. Table 1 gives the pertinent parameters of the experimental setup. The outputs of the Symbol Synchronizer Assembly (SSA) which are made use of are the integrated noisy symbol stream and the symbol transition clock. Sampling the integrated waveform at the bit transition corresponds to the integrate/dump or matched filter output. This sampling takes place in the suitcase interface. The samples are then recorded on magnetic tape by the 930 computer and also bit error tests are made on both S- and X-band data streams. A complete description of the suitcase, bit error counters, and recording process is contained in Appendix A.

B. Derived Signal-to-Noise Ratios

The performance measure used throughout the experiment is the received signal-to-noise ratio (SNR) of the S- and X-band data channels. In order to get several independent measurements of the SNR's, a variety of measurements were required and are listed in Table 2.

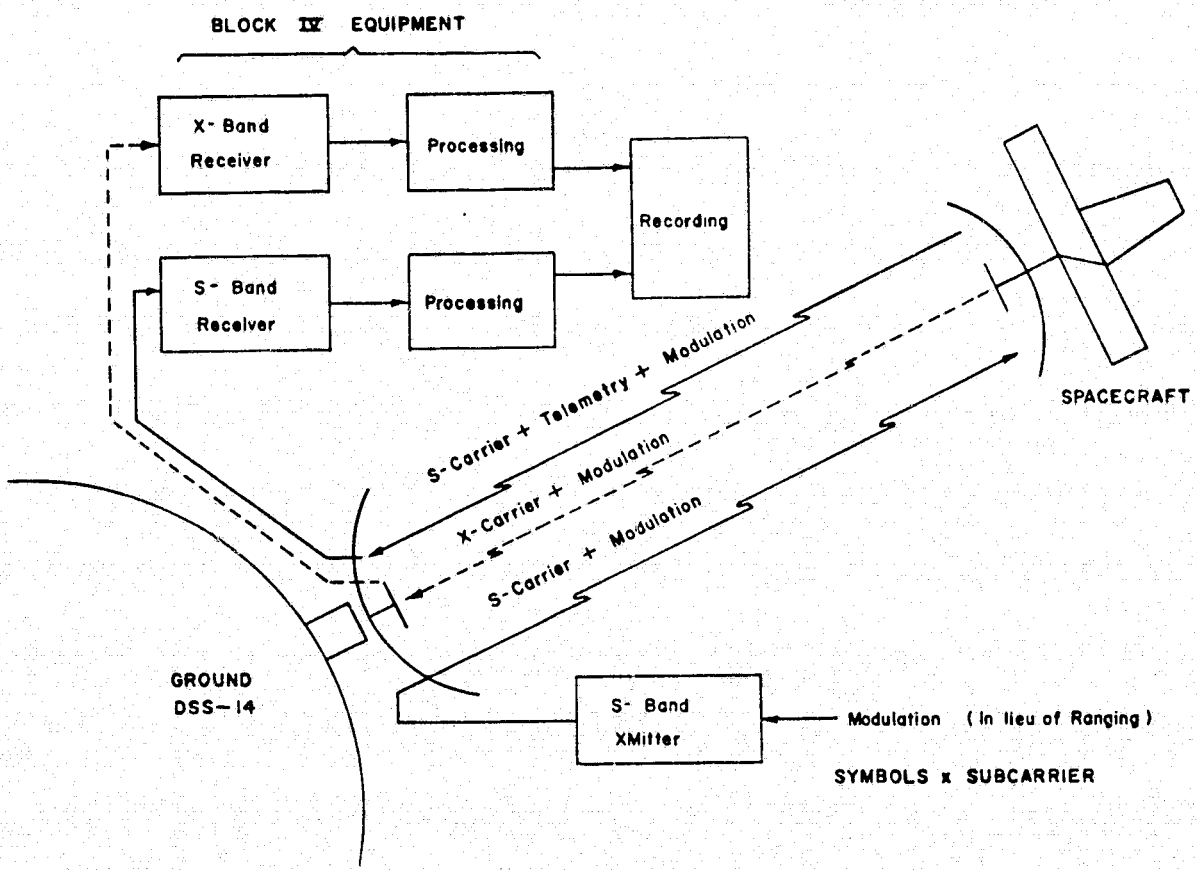

Fig. 1. Basic experiment configuration

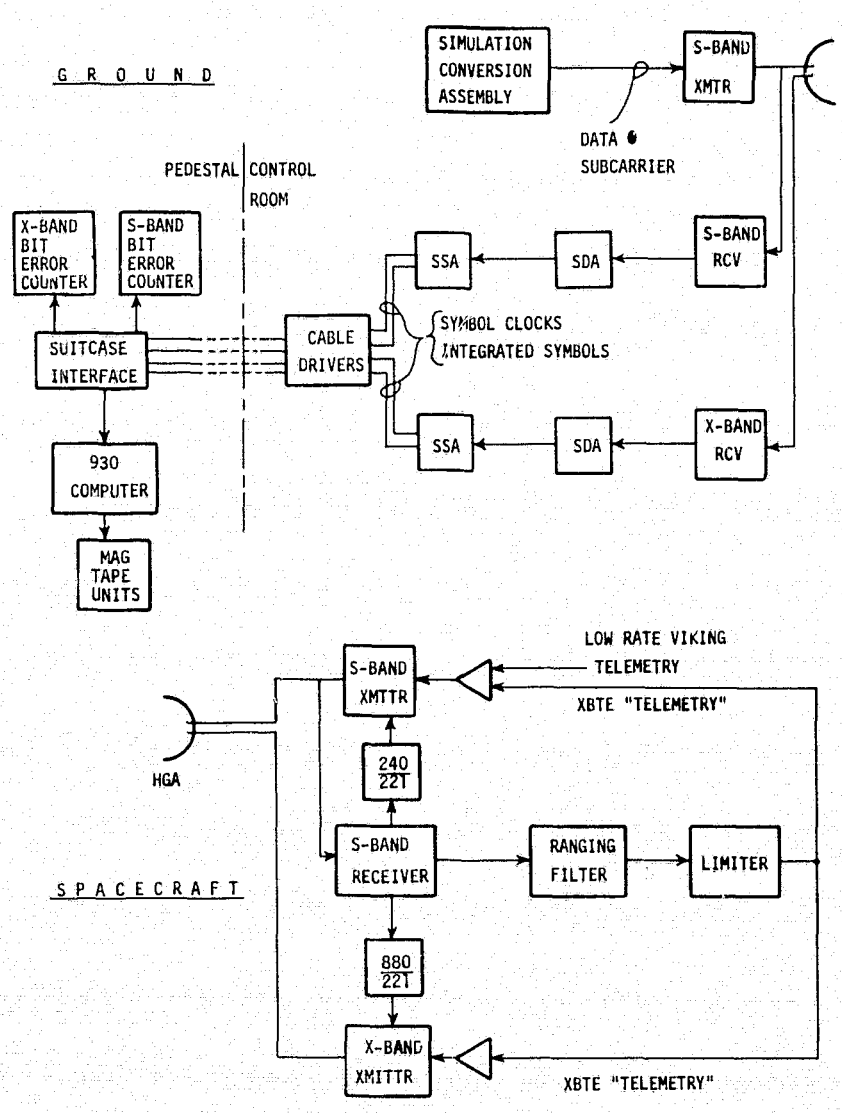

Fig. 2. Equipment block diagram

Table 1.

EXPERIMENTAL PARAMETERS

Data Symbol Sequence (NRZ)	111010
Data Rate	Variable
Subcarrier Type	Squarewave
Subcarrier Frequency	240,000 Hz
DSS-14 Transmitter Power	10 KW
Ranging Modulation Carrier Suppression	9 dB
Viking Command Modulation	On
Viking Low Rate (Engineering) Modulation	On (33 bps)
SSA Matched Filter Quantization	Sign plus 5 bits magnitude
Dates of Five Successful Passes (GMT):	Dec. 11, 1975 - Day 345
	Dec. 23, 1975 357
	Jan. 14, 1976 14
	Jan. 16, 1976 16
	Jan. 17/18, 1976 17/18

Table 2.

List of Experimental Data Sources

Periodic recording of symbol bit error rate.

Continuous recording of Symbol Synchronizer Assembly integrate/dump values and symbol clock.

Received signal strength from AGC (S- and X-band).

Real time recording of S- and X-band System Noise Temperature (T_{op}).

SNORE calculated by station Telemetry and Command Processor (S- and X-bands).

Antenna elevation angle.

Weather - predicted and actual.

X-band radiometer recordings (DSS-13).

Predicted S/C and ground parameters from Viking Orbiter Performance Analysis Group (OPAG).

Telecom Development Lab compatibility tests.

A brief description of each of the four SNRs derived from these measurements follows. (Complete detailed descriptions of these SNRs and the measurements are contained in Appendix A).

(1) P_E SNR

This SNR was derived from the measured bit error rate. The assumption made in this case is that the data signals are corrupted by additive white Gaussian noise. This implies no system nonlinearities or unusual signal interference. The SNR is thus related to the measured probability of error (P_E) by the standard PSK performance curve. The P_E measurements were taken for both S- and X-bands at regular intervals throughout each pass.

(2) XBTE Signal-to-Noise Ratio Estimate (SNORE)

A direct estimate of the signal-to-noise ratio can be made from the outputs of the integrate/dump circuits of the XBTE equipment. This involves a calculation of the mean and variance of the integrate/dump values multiplied by the true data (+1 or -1). These required sample values are recorded in real-time by the 930 computer on magnetic tape. The derived SNORE values were processed from these tapes at a later time.

(3) P_C/N_0 SNR

This SNR is calculated from measured values of the received carrier power, P_C, and the noise power density, N_0. The signal power is derived from the receiver AGC while the noise power density is derived from the system noise temperature (T_{op}) measurements. Both these measurements are real-time recordings on both S- and X-bands.

(4) TCP SNORE

This SNORE is calculated by the station's Telemetry and Command Processor (TCP) and is recorded every minute on the line printer in the station control room.

(5) Predict SNR

The predicted SNR is calculated in the same form as the P_C/N_O SNR using predicted values of received carrier power and noise power density obtained from the Viking Orbiter Performance Analysis Group (OPAG).

III. Experiment Results

While a total of 11 passes were originally scheduled for the experiment, a number of them were cancelled or unsuccessful for a variety of reasons described in Appendix B. Five of the passes, however, were successful; these occurred on December 11, 1975 (Day 345, GMT), December 23 (Day 357), January 14, 1976 (Day 14), January 16 (Day 16) and January 17/18 (Day 17/18). Table B1 of Appendix B lists the pertinent information relative to these five successful dates.

The data recorded on these passes was reduced and processed as uncoded data. The various predicted and estimated SNRs described in the last section are plotted in Figures 3-8 for X-band and Figure 9-14 for S-band. In these figures, some curves are missing because data required for their calculation were not available. Since the bulk of the quantitative results are contained in these figures, a number of comments follow which help interpret their meaning and significance.

1. All of the SNR plots track each other in terms of relative SNR vs time for a given pass. This is particularly evident on X-band where spacecraft antenna pointing can produce substantial fluctuations in SNR. The significance of this is that the relative performance of X-band telemetry can be determined from the T_{op} and AGC measurements which can be made on any normal X-band track. That is, future statistics could be accumulated during normal Viking X-band ranging passes.

2. The absolute difference between the SNR recordings is attributable to a number of factors, most of which are discussed in Appendixes A and C. The appropriate tolerances for the individual SNRs can be summarized as follows:

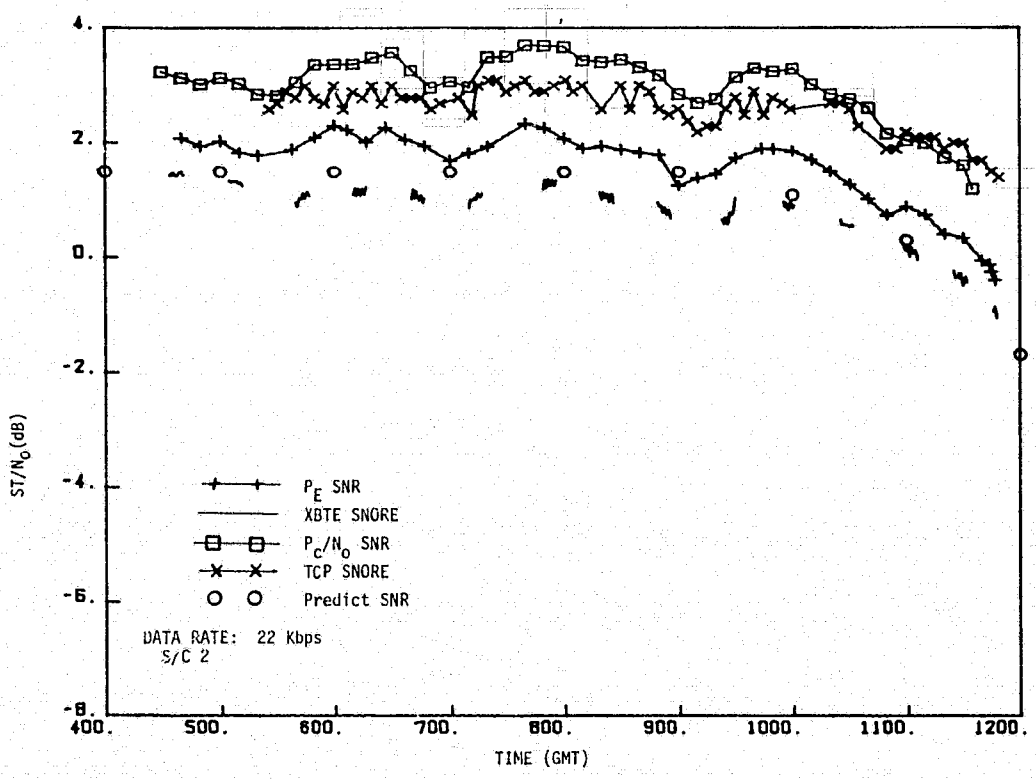

Fig. 3. X-band SNR, Day 345

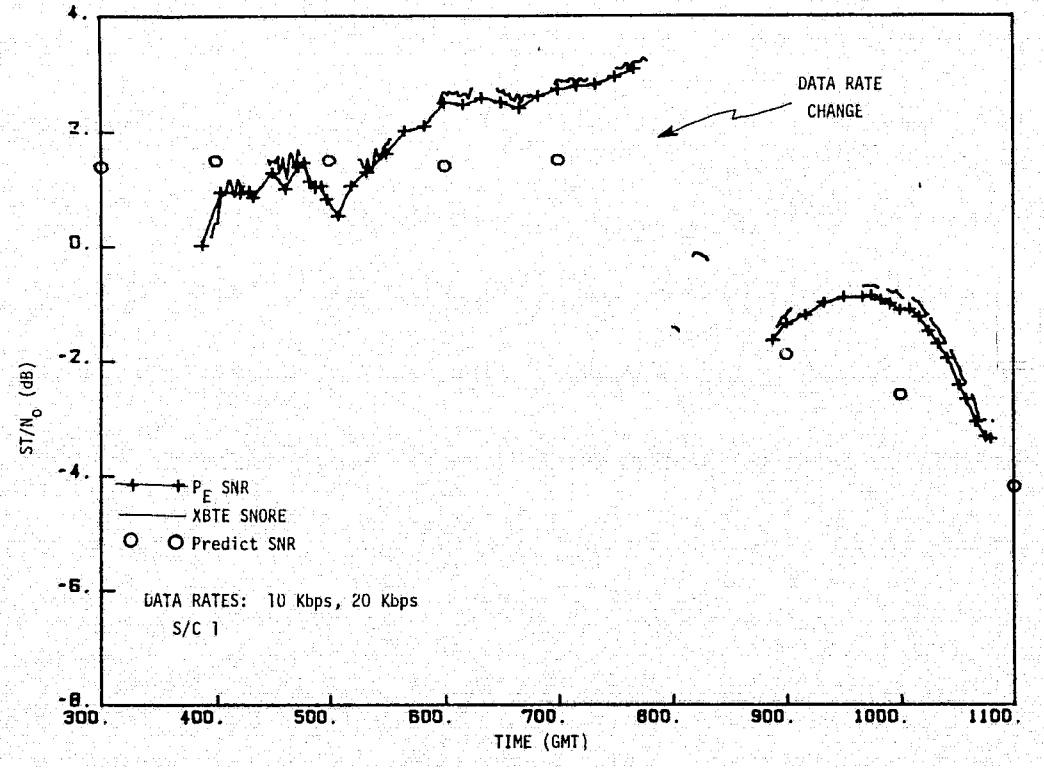

Fig. 4. X-band SNR, Day 357

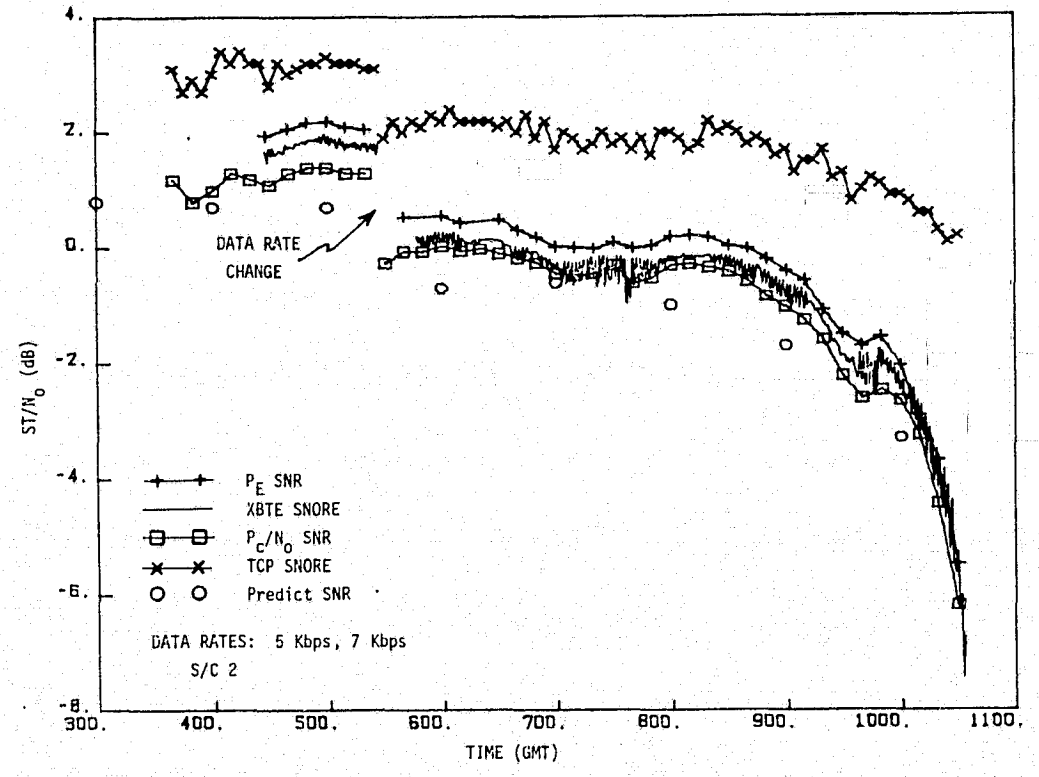

Fig. 5. X-band SNR, Day 14

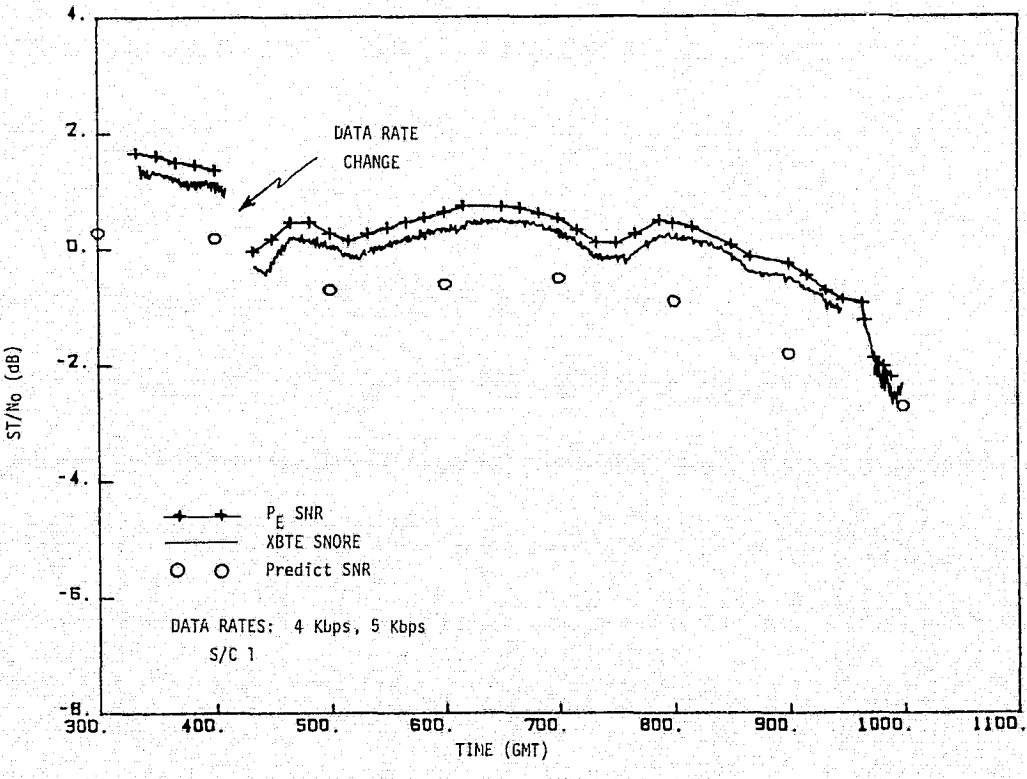

Fig. 6. X-band SNR, Day 16

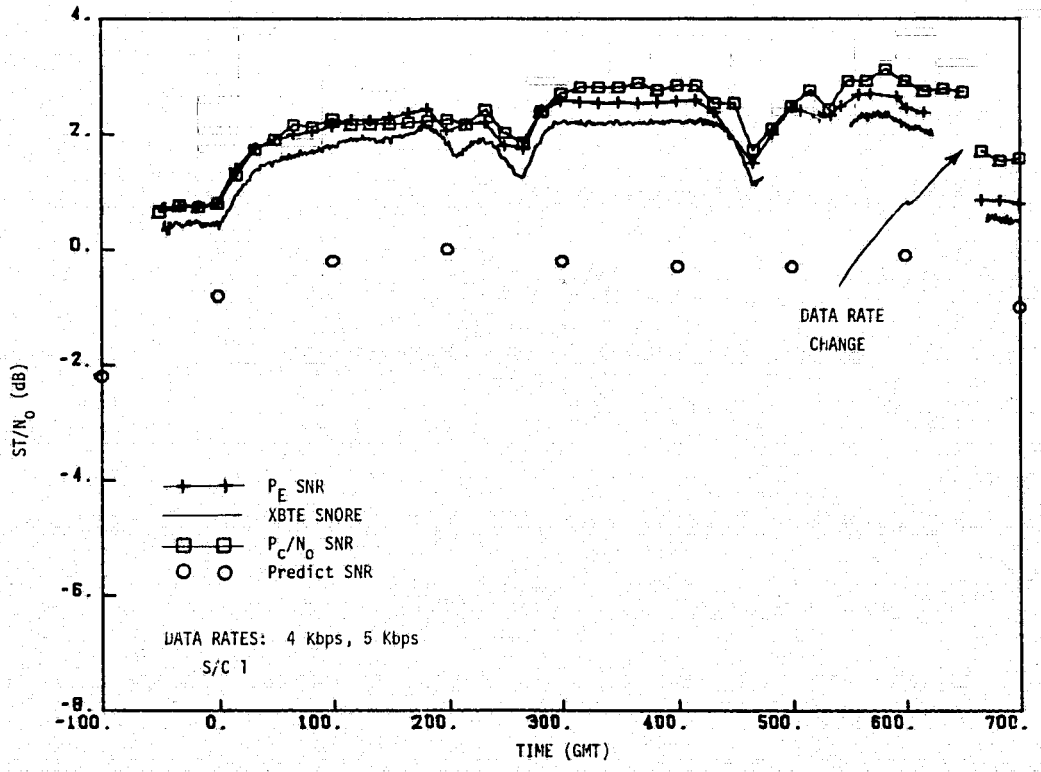

Fig. 7. X-band SNR, Day 18

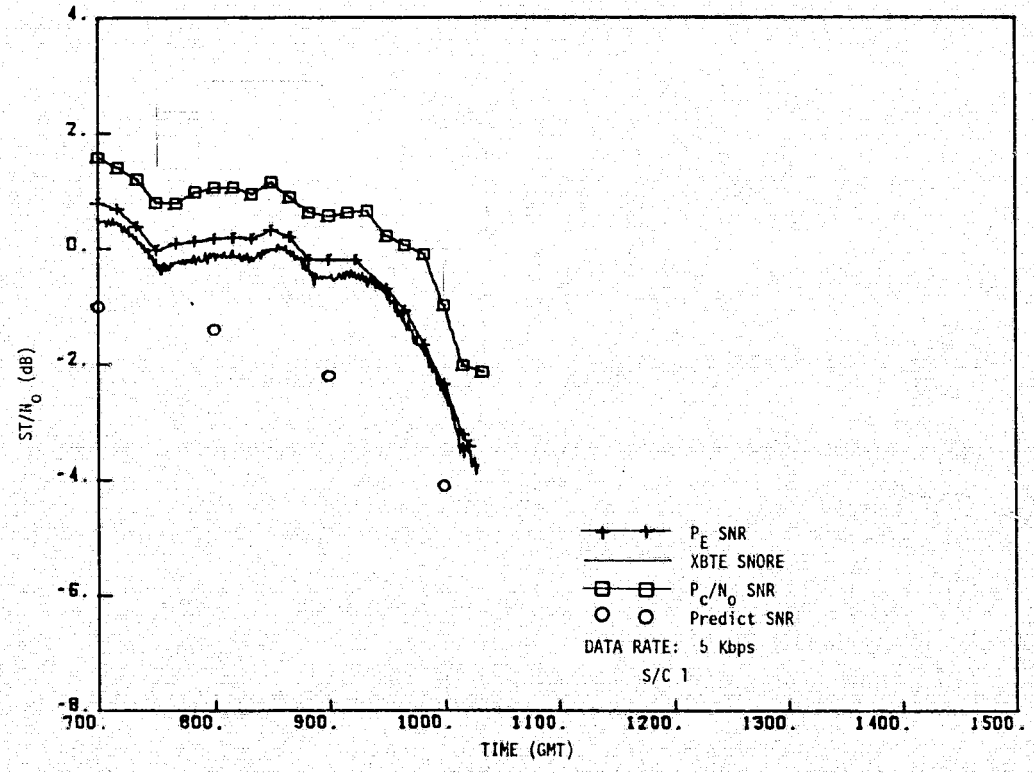

Fig. 8. X-band SNR, Day 18 (contd.)

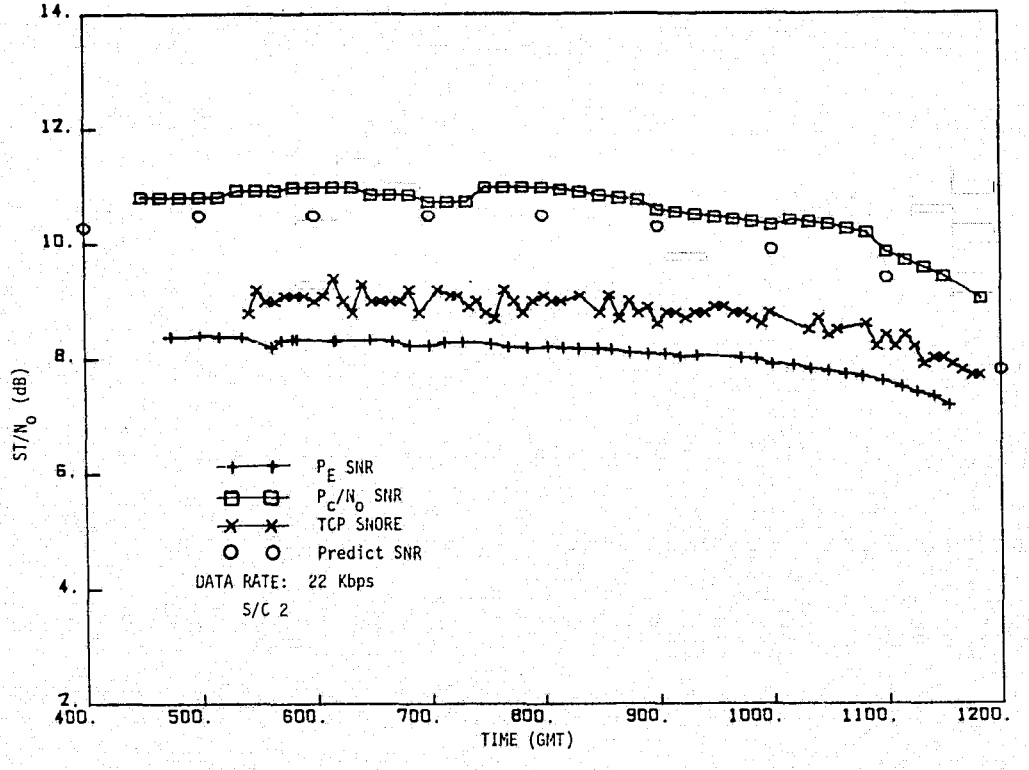

Fig. 9. S-band SNR, Day 345

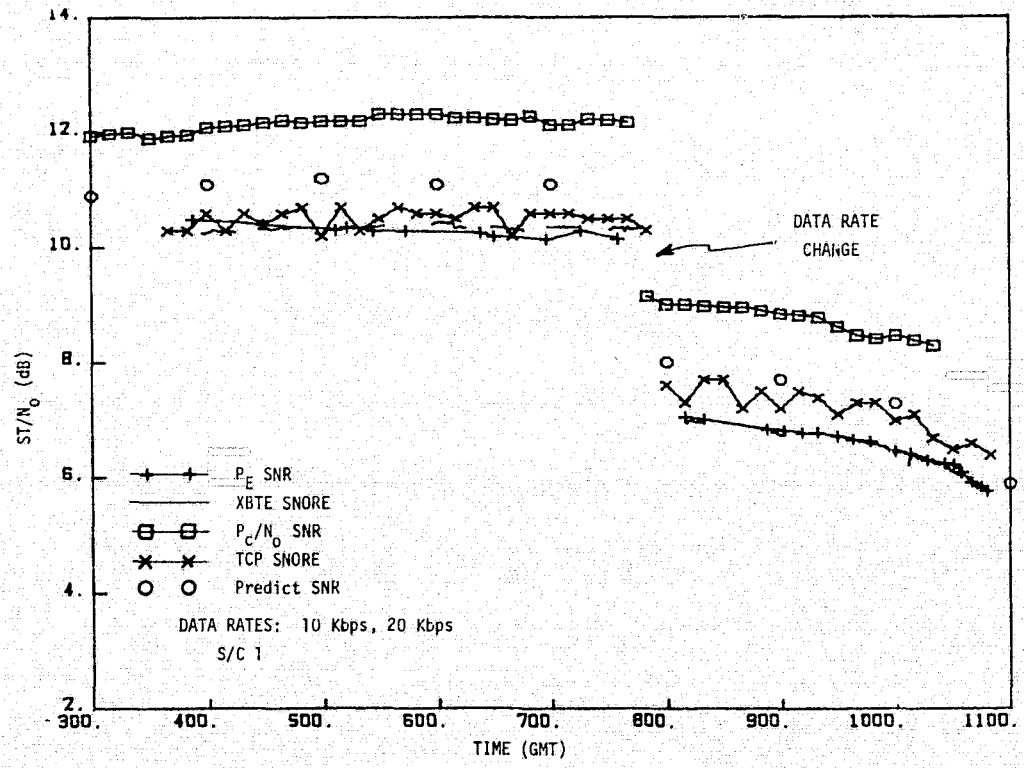

Fig. 10. S-band SNR, Day 357

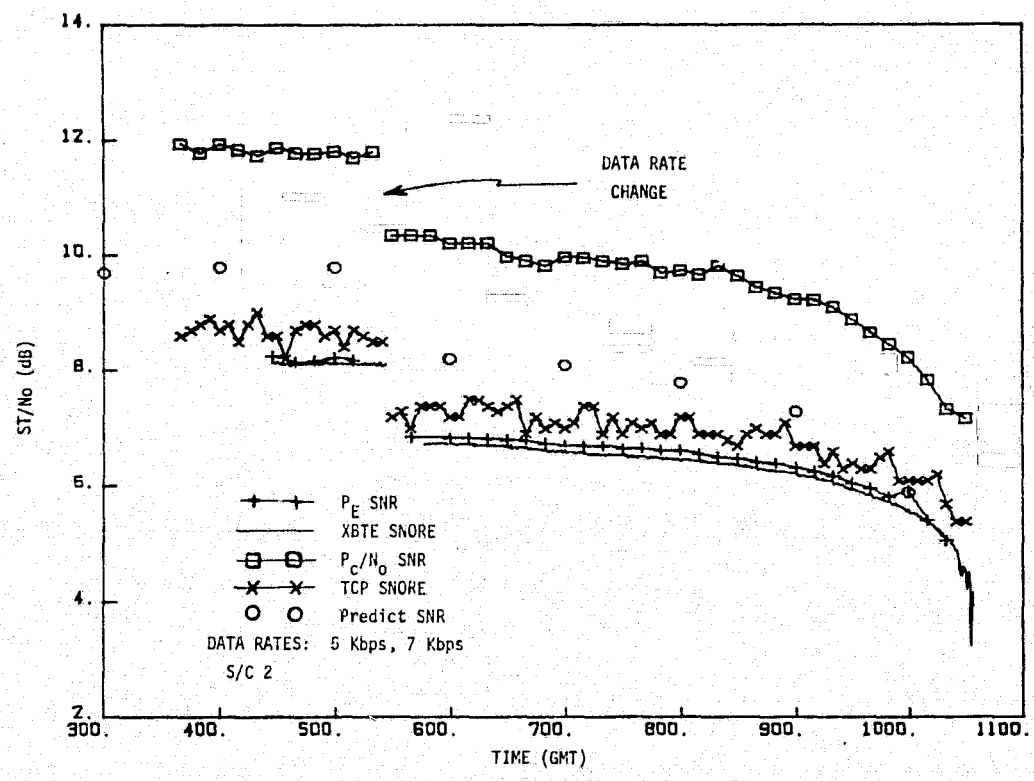

Fig. 11. S-band SNR, Day 14

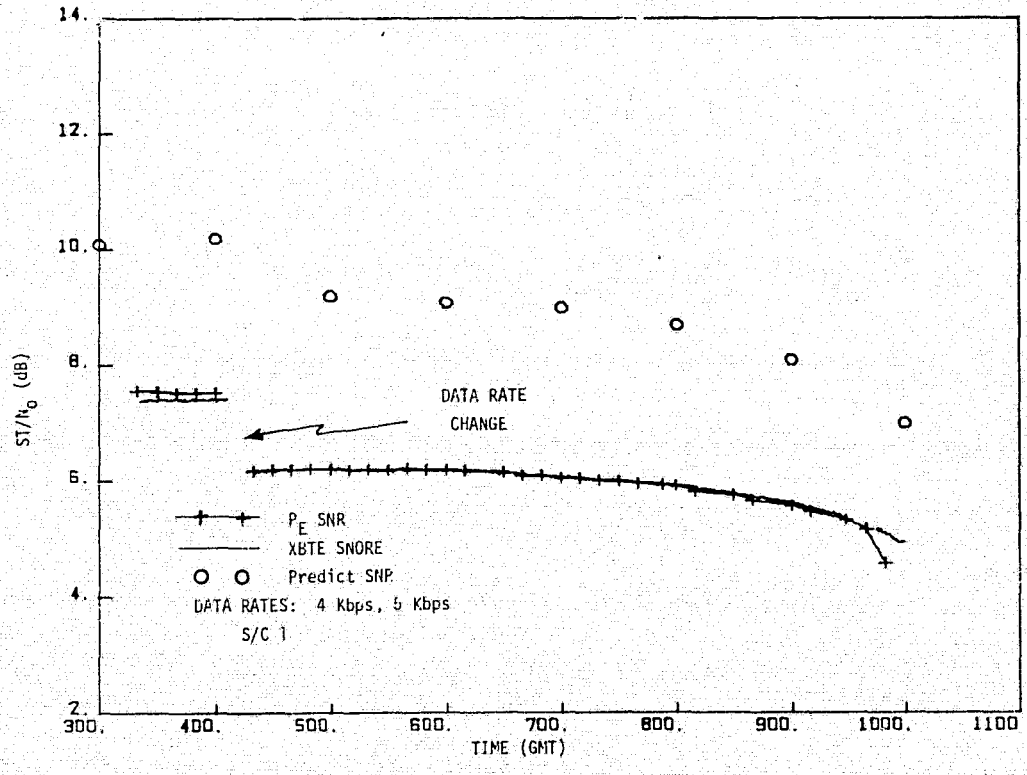

Fig. 12. S-band SNR, Day 16

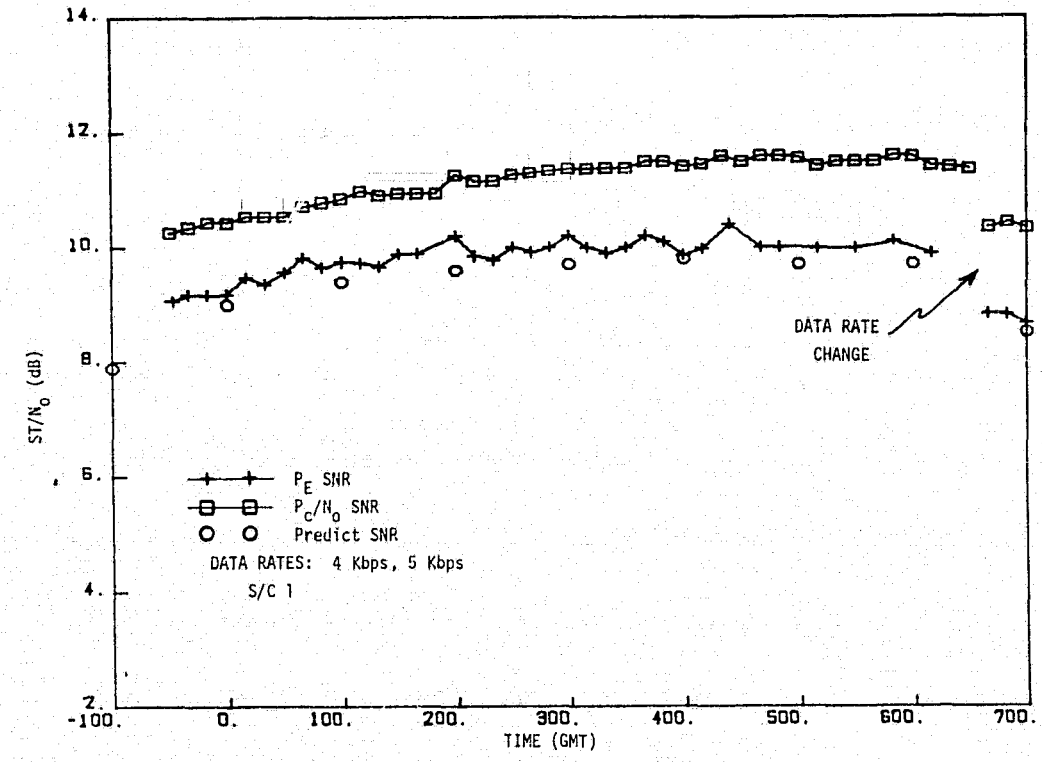

Fig. 13. S-band SNR, Day 18

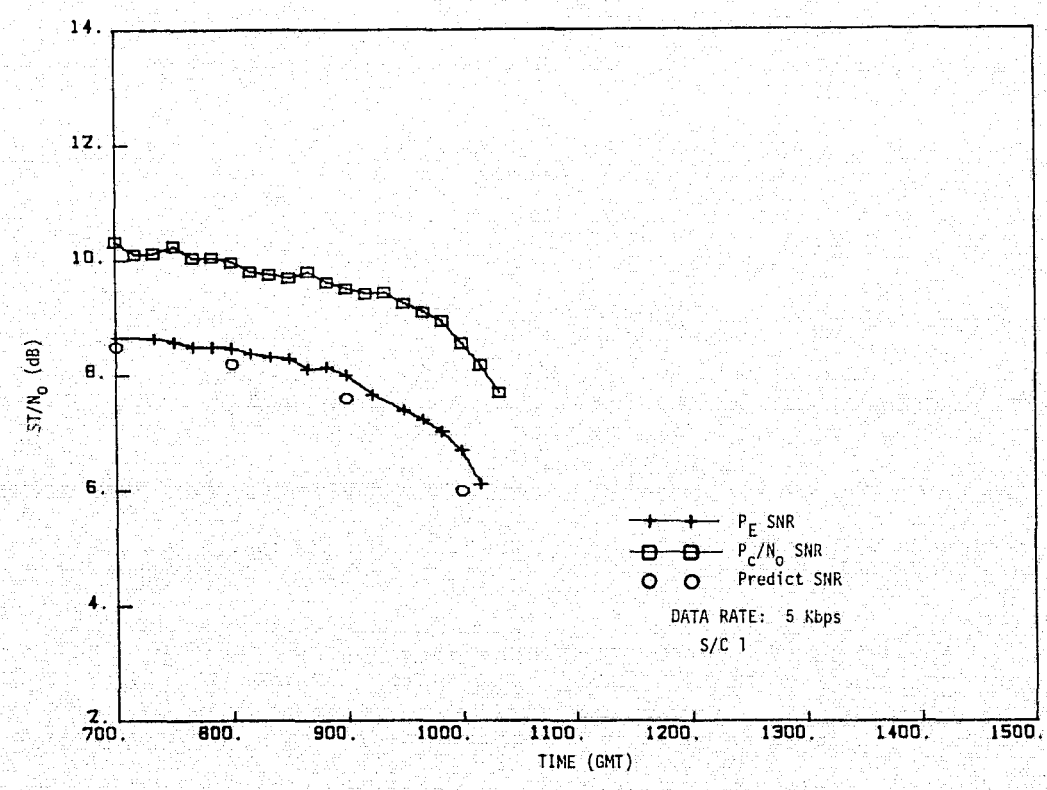

Fig. 14. S-band SNR, Day 18 (contd.)

P_E SNR	+0., -1.1 dB
XBTE SNORE	+0.3, - 0.5 dB relative to P_E SNR
P_C/N_O SNR	+4.8, -4.4 dB (X-band) +3.5, -3.0 dB (S-band)
TCP SNORE	$\pm$.5 dB
Predict SNR	+5., -6. dB

The point to be made is that nothing in the measured data was outside the expected tolerances. Stated another way, the experiment did not uncover any anomalous behavior in either the S- or the X-band systems. The interesting fact is that the absolute differences appear to be greater in the S-band case.

An indication of the relative and absolute differences between the P_C/N_O SNR (based on T_{op} and AGC recordings) and the P_E SNR are shown in Figures 15 and 16 for X- and S-bands respectively. The fact that the curves are roughly constant throughout each pass indicates that the two SNR's have the same relative shape. Note that the greatest standard deviation is only 0.4 dB. The mean, on the other hand, is an indication of the absolute difference between the two. As noted earlier, the S-band means are substantially greater than that for X-band. Two possible explanations exist for the large S-band discrepancies. First of all the S-band SNR was usually on the order of 10 dB. This means that the noise does not dominate such imperfections in the data recording, such as d.c. offsets, 60 Hz or other interference or noise, etc., as it would at 0 dB which was the typical SNR at X-band. Second, the very strong signal present in the S-band T_{op} measurement adds to the measurement of the noise power. While this was accounted for in the SNR calculation, it is not clear that its total effect was eliminated. Other

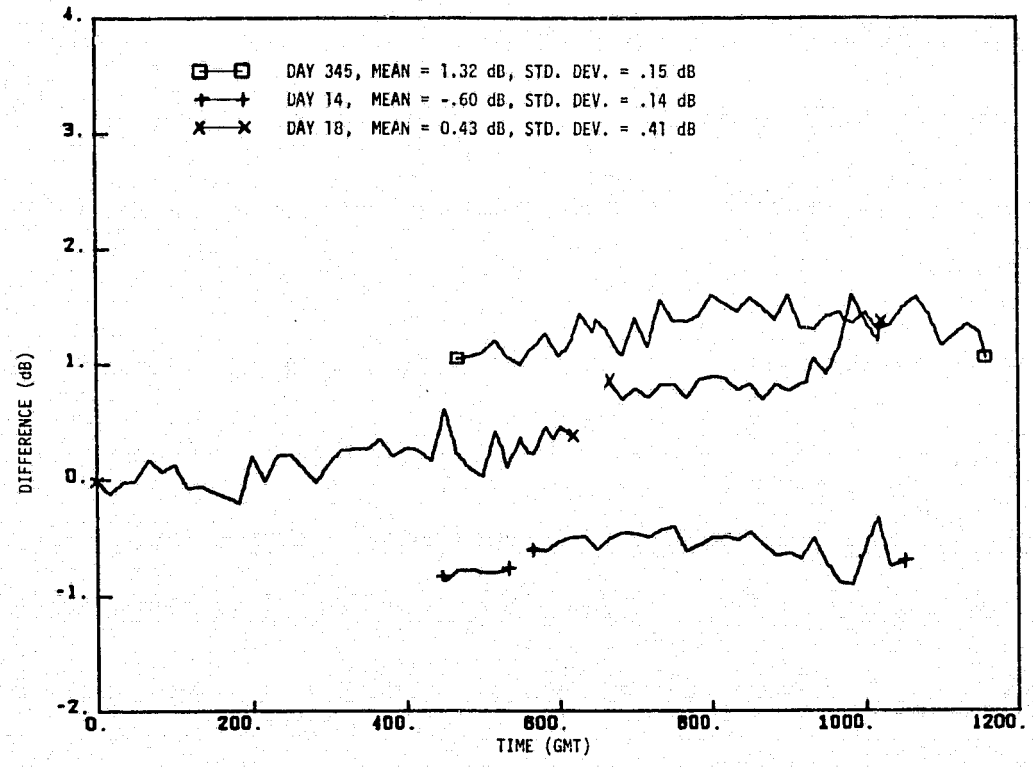

Fig. 15. Difference between P_c/N_0 SNR and P_E SNR (X-band)

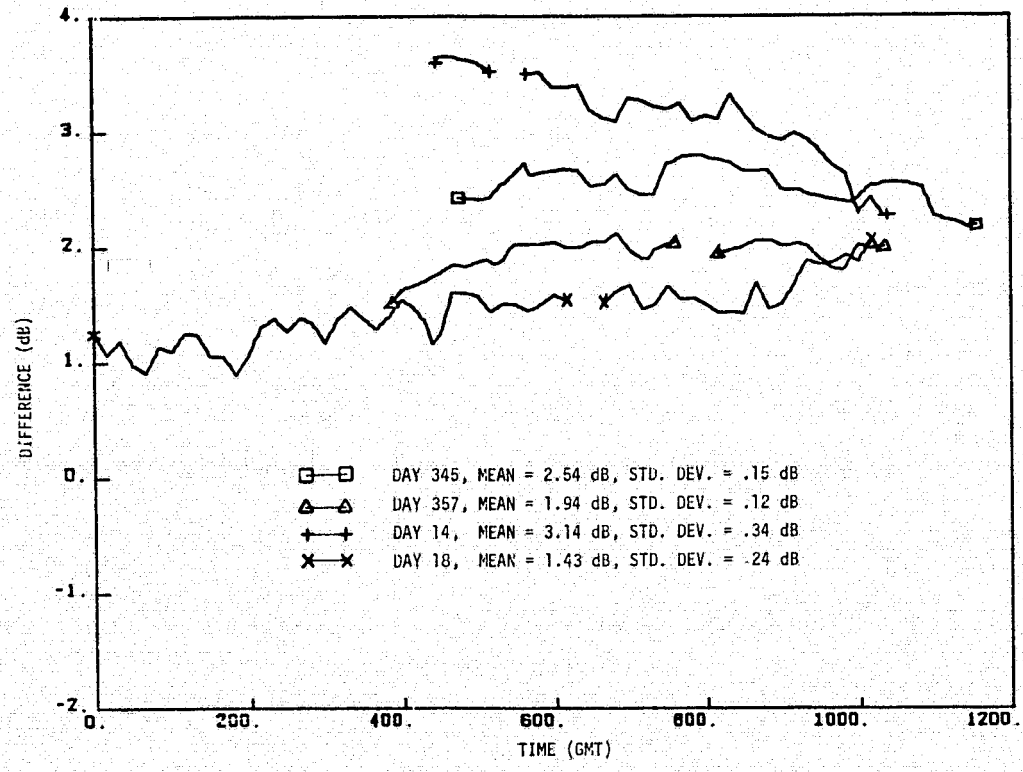

Fig. 16. Difference between P_c/N_0 SNR and P_E SNR (S-band)

possible problems are discussed in Appendix A.

3. The difference between the P_E SNR and the XBTE SNORE is explained in Appendix C. This problem, which was unanswered following the MVM XBTE[1], results from the improper setting of the amplitudes of the matched filter outputs prior to sampling. On day 357 the XBTE SNORE was actually slightly above the P_E SNR. Judging from this and the results of Appendix C, it seems safe to say that no unusual nonlinear effects are in evidence in the X-band telemetry string.

4. None of the cyclic variations in SNR which were present in the MVM experiment were noted in this experiment. As expected, little variation in S-band SNR occurred throughout the passes, while the X-band variations are most likely due to the spacecraft limit cycle motion. In fact, the X-band variations on day 345 correlated well with values of limit-cycle induced pointing loss which were calculated for a part of that pass (see Figure A6).

5. The fact that the SNRs track the shape of the predicted SNR indicates that the X-band predictions for station antenna gain and noise temperature as a function of elevation angle are relatively accurate. Measured X-band SNRs are equal to or above predicted values in all cases, and the measured values are within the tolerances of the predicted values. Thus, the predicted X-band SNR is reliable, at least for the clear weather case.

Several of the goals of the experiment, as stated in the Introduction, were either not met or have not been completed. No weather dependence on the X-band data was obtained because no substantial weather variations occurred during the passes. A possible source for weather dependent performance is suggested in the Conclusion section. No high rate (100 Kbps) data was taken

because the spacecraft was too distant by the time of the experiment period. It seems, however, that this is merely a high rate test of the Block IV equipment which could be accomplished with the test translator at the station or in CTA-21 at JPL. The coded performance (including compressed data experiments) is a matter of processing the recorded mag tape data. This will be done in time, funds permitting.

IV. Conclusions

The major conclusion of the experiment is that X-band telemetry works as expected. No anomalous behavior was noted during any of the passes of the experiment. No operational difficulties were uncovered. The existing X-band SNR prediction models provided reliable estimates of the average SNR for the clear weather cases, and the measured variations correlated with limit cycle induced pointing loss.

The major incomplete objective of the experiment was to study the dependence of X-band performance on weather. Because of the close agreement between the P_E SNR and the P_C/N_0 SNR, accurate estimates of X-band telemetry performance can be obtained from SNRs derived from T_{op} and AGC measurements. In this experiment, the largest uncertainty in the P_C/N_0 SNRs resulted from inaccuracies in the T_{op} measurements. To reduce these uncertainties and to simplify T_{op} measurement procedures, it is strongly recommended that an automatic measurement system be installed to record and calibrate the system noise temperature during all X-band operating periods. In the low temperature DSN system, a weather-induced change in T_{op} affects X-band performance much more than the corresponding change in AGC. Thus, accurate measurements of X-band T_{op} are necessary to obtain accurate models of the weather/performance relationship.

REFERENCE

1. Springett, J.C. and F. J. Kollar, "Results of the MVM'73 X-band Telemetry Experiment," Document 615-149, Jet Propulsion Laboratory, Pasadena, California, May 1974 (an internal document).

APPENDIX A XBTE SNR Measurement Descriptions

A. Experimental Hardware

The general equipment configuration is shown in Figure 2 in the text of this report. The signals required for the experiment were extracted from the Symbol Synchronizer Assemblies (SSAs) located in the control room of the station. These signals consisted of the channel A integrator, channel B integrator and the symbol clock, which were extracted from both the S- and X-band SSA. These signals had to be preconditioned and sent to the XDS 930 Computer in the pedestal of the antenna, some 500 feet away.

The channel A and channel B integrators, integrate and dump over alternate symbol periods. They were fed into a summing cable driver (Figure A1) resulting in a composite integrate and dump signal being received at the computer interface. The symbol clocks were fed into Schmitt trigger circuits followed by cable drivers (Figure A2) and sent to the computer interface.

The computer interface is a self-contained electronic package mounted in a suitcase to provide portability (Figure A3, A4). Functionally, the suitcase digitizes the integrate and dump signals into 6 bit (including sign) binary representations, and packs these into a 24 bit computer word. The format of the packed computer word is:

> The 6 most significant bits contain an S-band sample, the next 6 bits contain an X-band sample, the next 6 bits contain the next S-band sample and the 6 least significant bits of the word contain the next X-band sample.

The inputs to the suitcase consist of the S- and X-band composite integrate and dump signals, and their respective symbol clocks. These four signals are fed into cable terminators, the outputs of which are tied to the proper input modules.

The symbol clocks are used as convert pulses in analog to digital (A/D)

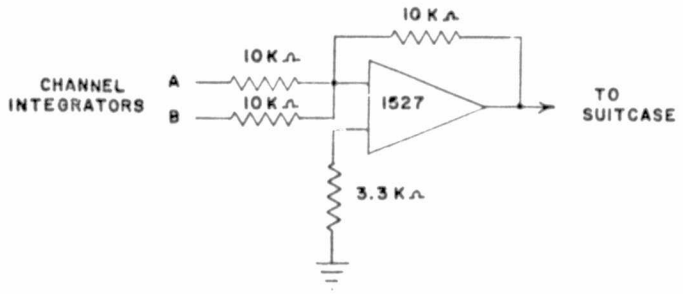

Fig. A1. Summing cable driver

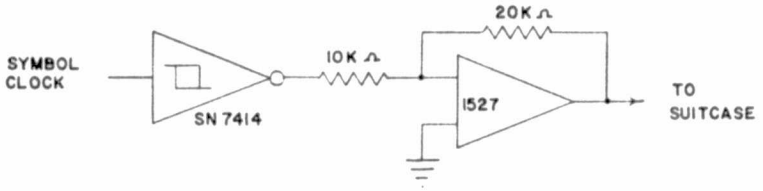

Fig. A2. Clock cable driver

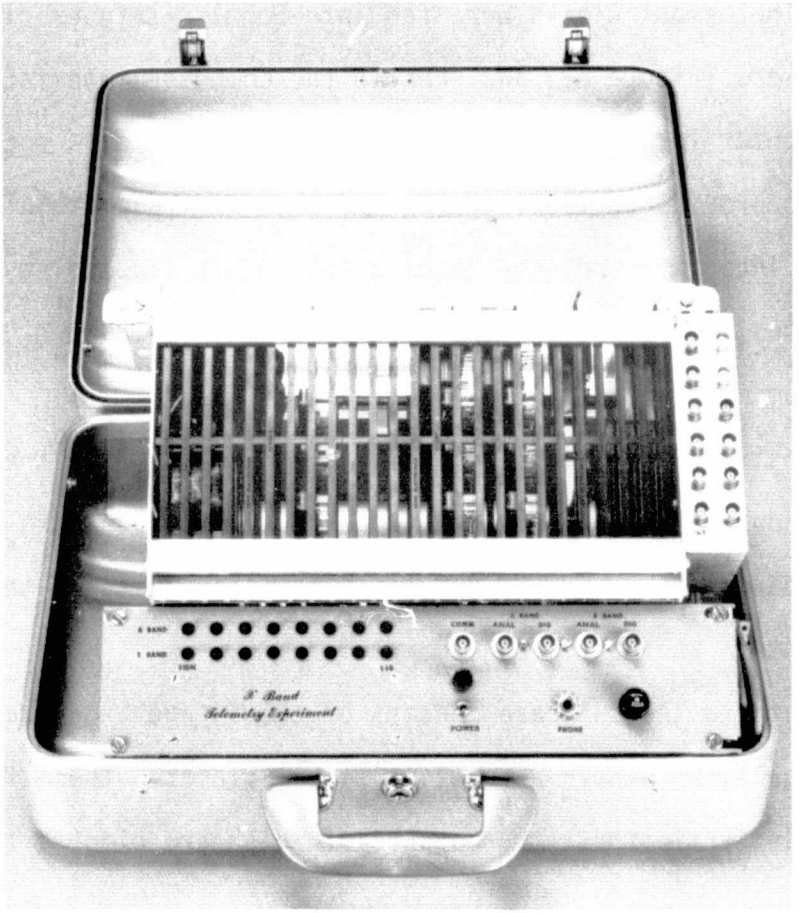

Fig. A3. Computer interface suitcase

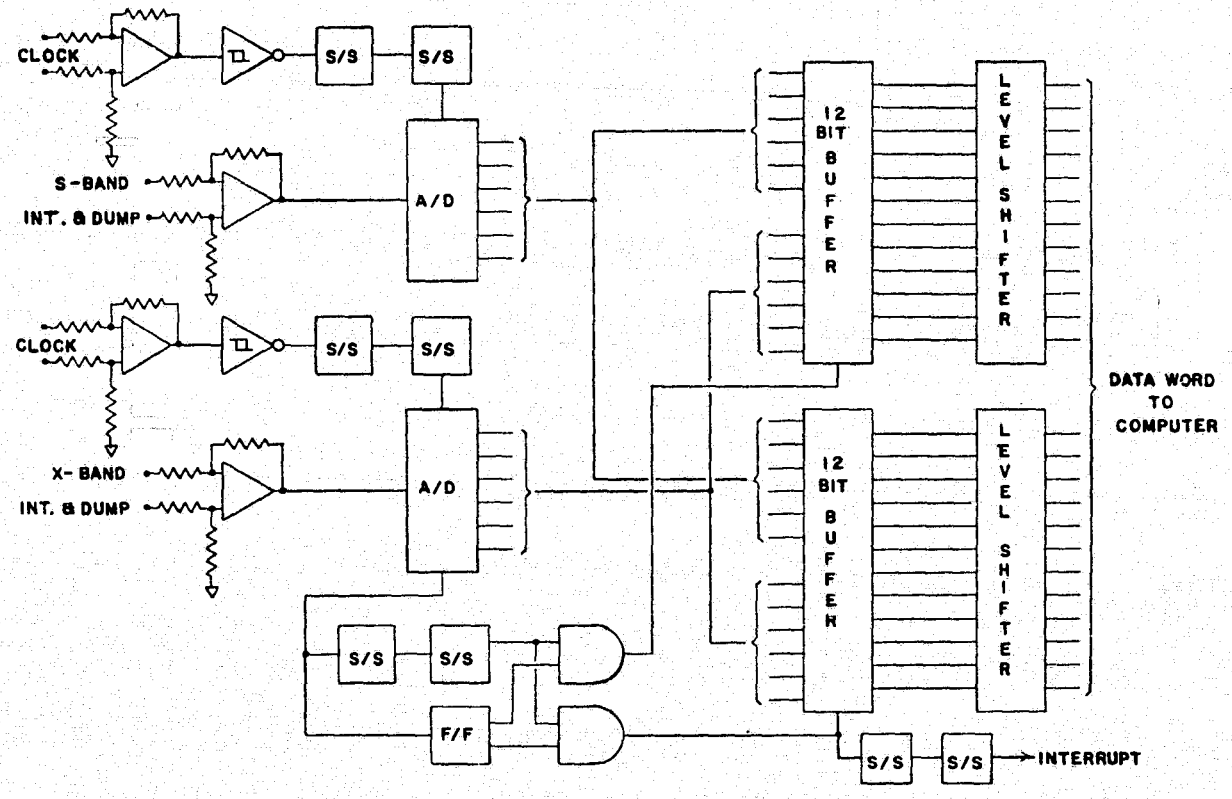

Fig. A4. Block diagram, computer interface

converters. They are reshaped by Schmitt trigger circuits and fed into serial pairs of single shots, thus allowing for adjustable convert pulse widths and the ability to position the pulses (in time) so that the A/D converters are sampled at the correct time instants.

The integrate and dump signals are fed into high speed sample and hold circuits, which in turn feed the analog inputs of the A/D converters. The sampling occurs just prior to the dump. The digitized S-band sample is bussed to the 6 high order bits of low 12 bit holding registers and the digitized X-band sample is bussed to the 6 low order bits of these registers. The 12 bit holding registers form the packed 24 bit computer word and are loaded alternately after each X-band sample. After the low order register is loaded, an interrupt is issued to the computer, which in turn accepts the contents of the 24 bit register after they have passed through a logic level shifter making the logic levels compatible with the computer.

Aside from furnishing the 930 computer with the complete 6 bit samples of the integrated symbols, the suitcase also provides the detected data (sign bit) and symbol clock which are used for bit error counting. Two bit error counters (one each for the S- and X-band data streams) are used to provide a continuous real-time monitoring of the probability of error. In lieu of using the transmitted data for comparison, a sequence generator was designed into the bit error counter which can be preset to any sequence. The detected data and the transmitted or internally generated data are passed through pairs of inverters for shaping and buffering, and through a 4 bit fixed delay for proper alignment with the clock. The input to the fixed delay in the transmitted data leg is switched to input either data or its complement in case the detected data is complemented by the SSA's. The output of this fixed delay is fed into a switch selectable delay allowing for proper alignment of

the data stream to be compared. The outputs of the selectable delay and the fixed delay in the detected data leg are fed into the bit comparator circuitry which outputs 3 signals, one for each comparison (total bits compared), another for the bits in error and another for the 1's in error. These 3 signals are fed into their respective displays.

The clock is passed through an inverter for shaping and buffering to a switch which passes the clock or its complement to the input of an AND gate. The AND gate is controlled by Reset/Start button and the Stop Count Signal from the Total Bits Compared Display. When the Reset/Start button is depressed, a signal is sent out to reset and clear the 3 displays, the Stop Count signal is set high and the clock AND gate is enabled. The bit by bit comparison of the 2 data streams will continue until a switch selectable total bit count is reached; at this time the Stop Count signal goes low disabling the clock AND gate.

B. Software

The computer program for gathering data operates in real time under interrupt control. It was written in XDS Symbol, an assembly language for XDS 9-series machines. The program alternately filled one of two 6000 word arrays; as one array was being filled, the other array was written out onto one of two magnetic tape units. As described in the previous section, each 24-bit computer word contained two 6-bit S-band samples and two 6-bit X-band samples. The magnetic tape units were switched from one to the other by the program, as their tapes became full. This alternating process results in a contiguous data stream being gathered.

Another program was used to process the uncoded data on these tapes in non-real time. After acquiring the appropriate six-bit data sequence for each tape, this program computed the probability of error and SNORE for each minute of recorded S- and X-band data.

C. P_E SNR

During the experiment passes, the probability of error (P_E) was calculated using the results of the bit error counters (Figure A5). Typically 10^6 symbols were used to calculate P_E for X-band and 10^7 for S-band which always had the higher SNR. These calculations were performed roughly every 10 minutes throughout each pass. If the ideal white Gaussian noise channel is assumed, then the corresponding symbol SNR can be calculated as

$$SNR = [\text{erfc}^{-1}\ (2P_E)]^2$$

These SNR values are plotted in Figures 3-14 in the text of this report.

There are a few sources of error in the experiment which can degrade the P_E measurement. A d.c. offset in either the cable drivers, sample/hold or ADC could produce an error. An attempt was made to keep these balanced. Also, included in the bit error counters were 1's in error counters; that is, a count of the number of errors when the true data was a "one." Since 2/3 of the symbols in the symbol sequence are "ones," it is expected that the "1's in error" count be 2/3 of the total bit errors. Any d.c. offset would change this ratio. Since this ratio was maintained reasonably well, it is expected that the d.c. offset degradation is only on the order of -0.1 dB.

A more serious source of error is the alignment of the sampling of the integrate/dump waveforms. A 10% timing error could result in an SNR degradation of -0.8 dB.

Other sources of error such as 60 Hz and other interference, non-ideal sampling, etc. could account for perhaps -0.2 dB degradation. Thus, the total maximum expected degradation for the P_E measurement is about -1.1 dB.

D. XBTE Signal-to-Noise Ratio Estimate (SNORE)

The SNORE calculation is made in non-real time from the sampled matched filter values which were recorded on mag tape. This SNR estimate is

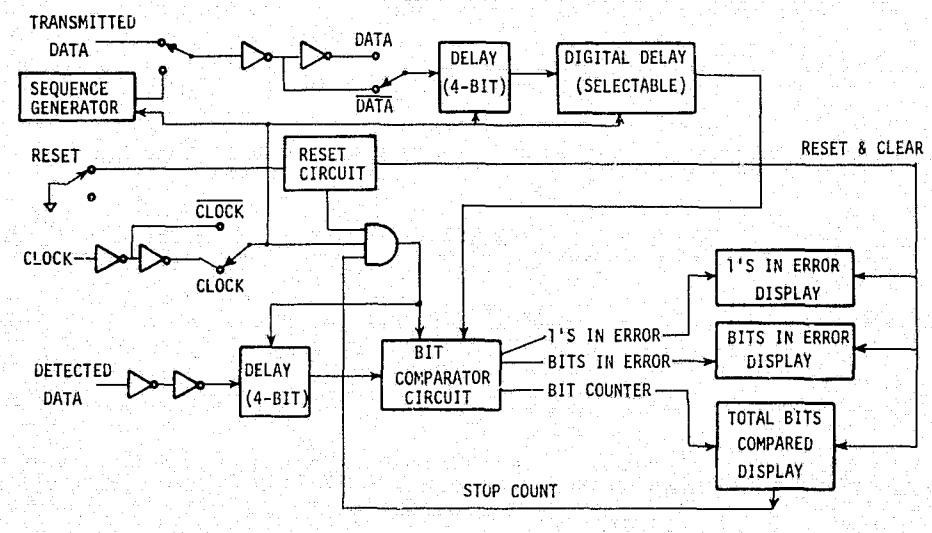

Fig. A5. Bit error counter

given by

$$\text{SNORE} = \frac{\text{MEAN}^2}{2 \times \text{VARIANCE}}$$

where

$$\text{MEAN} = \frac{1}{M} \sum_{i=1}^{M} y_i^2$$

$$\text{VARIANCE} = \frac{1}{M-1} \sum_{i=1}^{M} y_i^2 - \text{MEAN}^2$$

and the y_i are the quantized matched filter sample values multiplied by the true data (+1 or -1). For the plots of SNORE given in Figures 3-14, M was chosen such that the SNORE was calculated for one minute of data.

The sources of error given in the preceding section also apply to the SNORE values. In addition, another potentially great source of error is discussed in Appendix C. This pertains to the amplitude settings of the signals prior to sampling. Since no nonlinear effects were ever noticed (even the expected radio loss for these passes was predicted to be very small), the difference between the SNR curves derived from P_E and the SNORE curves is primarily attributable to this amplitude setting phenomonon.

E. P_c/N_o SNR

In this experiment, estimates of the SNR were calculated from measurements of the system noise temperature, T_{op}, and the receiver AGC.

Calculations of SNR may be made in two different forms:

$$(ST/N_o)_1 = M_1 TL_S L_A L_C L_{PR} P_{Tt} G_t G_r / N_o,$$

and

$$(ST/N_o)_2 = M_1 P_{cr} TL_{PR} / M_2 N_o$$

where M_1 = ratio of data power to total power,

T = bit time,

L_S = space loss,

L_A = atmospheric loss,

L_C = circuit loss,

L_{PR} = processing loss,

P_{Tt} = total S/C transmit power,

G_t = S/C transmit antenna gain,

G_r = ground receive antenna gain,

$N_o = k\ T_{op}$ = noise spectral density,

T_{op} = system noise temperature,

P_{cr} = ground received carrier power,

and M_2 = ratio of carrier power to total power.

During this experiment the second form of the SNR calculation was used because both the received carrier power and system noise temperature were available from measured data obtained during the experiment periods. These SNR calculations provided the ability to study separately the effects of the receiver carrier power and system temperature.

The received carrier power is obtained by converting the receiver automatic gain control (AGC) voltage into received carrier power. This conversion is performed by the DSN station computer system and the results are transmitted to the Project Telecom Analyst at JPL. The conversion from volts to dBm requires a calibration which is performed before a station pass. The relative relation (dBm/volt) is generally well known, while the absolute relationship (x volts = y dBm) must be calibrated before each pass because of equipment gain drifts and configuration changes which occur from day to day. If no calibration is made, the AGC relative accuracy over a pass will be good, but the absolute accuracy may be in error by a dB or more.

The system noise temperature was not directly available from the Block IV receiver system at DSS-14 because the system has no noise adding radiometer. Temperature data were derived from analog recordings of the total received power using a wideband detector. The total received power is a function of the received noise power, the total received signal power, and the maser gain. If the measer gain is constant and if the signal power is much less than the noise power, then the analog recordings give the values of noise temperature directly. The pre-pass calibration uses a Y-factor measurement and recording of the Zenith system temperature. Then the detector input is connected to an ambient-temperature (known) load and the corresponding recording is made. Since these are back-to-back procedures, the maser gain is assumed to be constant and, with no signal present, the scale factor (K°/inch) is readily obtained. This factor was usually about 50°K/inch. At the end of the pass, the detector input is connected again to the ambient load, but no Y-factor calibration is made. Any change in the ambient load voltage level indicates that the maser gain has drifted. The gain drift is assumed to be linear because no gain drift history has been obtained. Thus, a time-varying scale factor is obtained and the recorded voltage values can be directly converted to apparent system temperature. In this experiment, the total signal power level was comparable to the noise power level, so the total signal power, $P_{cr}M_2$, was subtracted from the measured total received power to obtain estimates of the system noise temperature. These calculations assumed a 12 MHz system bandwidth for both S- and X-band.

Reduction of the received signal level data involved hand-averaging of the receiver AGC values over 10-minute intervals. These printed data were obtained from the Viking Telecom Analyst. Reduction of the analog recordings to obtain noise temperature estimates was also done by hand. For each analog recording, the calibrations were calculated and the measured temperature values

were obtained at 10-minute intervals. Then the resulting temperatures and received signal levels were combined by machine with appropriate link parameters to obtain the estimates of the actual temperatures and SNRs.

The processing loss, L_{PR}, includes the ground system processing loss plus the spacecraft limiter suppression, which depends on uplink signal level. Values of these parameters, as well as the power ratios M_1 and M_2, were obtained for each experiment period from the Telecom Analyst of the Viking Orbiter Performance Analysis Group (OPAG).

The calculated values of SNR have many potential sources for errors. The receiver AGC calibration accuracy is the main error source of AGC error, while maser gain drift and station configuration uncertainties contribute most to errors in the temperature estimates. The noise power detection bandwidth estimate can cause relatively large errors when the signal level is high, as it was at S-band during the early experiment periods. Table A1 shows the major error sources and the estimates of the upper limit of their effect on the SNR calculations.

F. Predict SNR

The predicted SNR was calculated in the same form as the P_c/N_o SNR by replacing measured T_{op} and AGC values with the corresponding values predicted by the OPAG.

G. X-band SNR Variations Due to Antenna Pointing Loss

During the data analysis, variations were observed in the measured values of X-band SNR (see e.g. Fig. 3). These variations were assumed to be the result of S/C limit cycle induced pointing loss. Figure A6 shows a plot of the measured X-band AGC used to obtain the P_c/N_o SNR in Figure 3. Also shown in Figure A6 is a plot of X-band S/C antenna pointing loss for the same period of time. The pointing error angle vs. time was obtained from the OPAG, and then

Table A1.

SNR Calculation Error Estimates

Error Source	SNR Uncertainty (dB) S-Band	X-Band
AGC		
AGC Calibration Accuracy		
With pre-pass cal	±.2	±.5
Without pre-pass cal	± 1	± 3
Recorded AGC Data Resolution	±.1	±.1
Temperature		
Temperature Calibration Accuracy	+.5-0.	+.4-0.
Maser Gain Drift	±.5	±.5
Configuration Uncertainties	±.5	±.3
Temperature Recording Resolution	±.1	±.1
Power Detection Bandwidth	±.3	±.1
AGC Calibration Accuracy	±.3	±.1
Other		
S/C and Ground Parameters	±.2	±.2
Worst Case Total	+3.5-3.0	+4.8-4.4

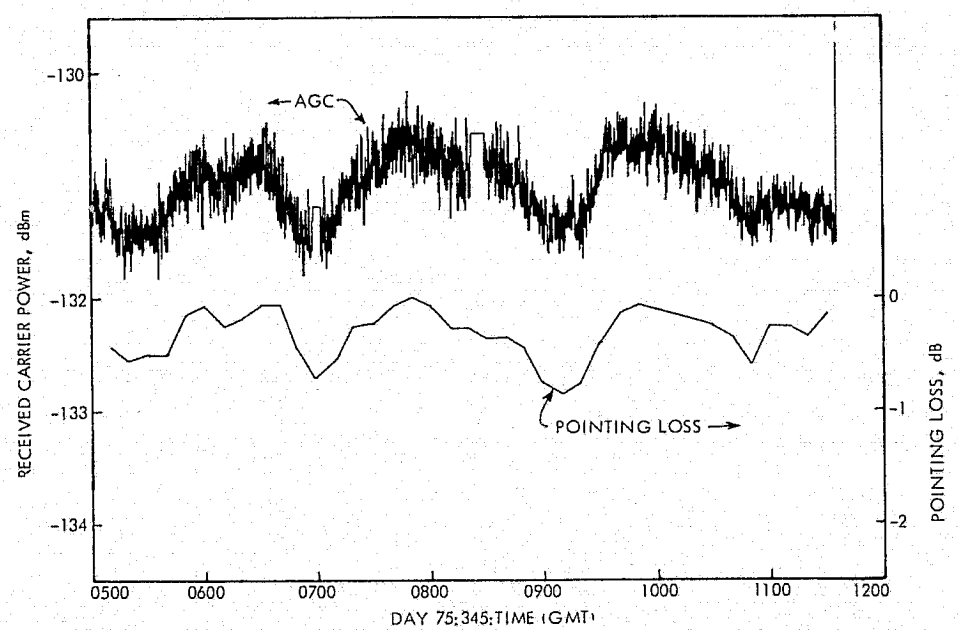

Fig. A6. Viking 2 X-band AGC and calculated pointing loss

the pointing loss was calculated using the X-band antenna pattern, also obtained from the OPAG. The two curves in Figure A6 are similar in all respects, so the observed cyclic variations in the SNR may be attributed to the S/C antenna pointing loss.

APPENDIX B

Viking XBTE Diary

The following is a diary of the significant events that took place prior to, during, and after the X-band telemetry dates. Included in this are problems encountered, successful measurements taken, times, dates, etc. Following this is a matrix of the five most successful experiment dates with the pertinent information (Table B1). All times and the day of year (DOY) are in GMT.

DOY (1975-6)

128 A compatibility test was run in Section 339's Telecommunications Development Lab (TDL) using the XBTE modulation as well as 33-1/3 Viking low rate telemetry. No interference was observed between the two modulations.

300 Review meeting attended by Section 339 Viking and MJS project personnel to approve plans of XBTE.

310-334 A number of meetings with DSN and Viking project personnel to achieve the following: (1) get DSN agreement to conduct XBTE on non-interference basis; at this point it appeared that XBTE could be cancelled because of DSS 14 scheduling of maintenance commitments, (2) convince DSN that pre-pass calibrations for XBTE did not require hours of time and were, in fact, simple, straightforward and had already been done for the MVM-XBTE, (3) get DSN to approve a temporary ECO to connect the already existing T_{op} and AGC strip chart recorder for X-band; this decision cost the XBTE experimenters a great deal of time and was frustrating because it was also needed for other X-band operations; (4) get the Viking Project to schedule passes for the XBTE at DSS 14. Note: Because of the tight scheduling at DSS 14, the very desirable dry run for XBTE was not possible.

328 Meeting with DSS 14 station personnel about XBTE impact on equipment changes, scheduling, etc. Everything seems in order.

328 Date of issue of ECO 75.110 - the XBTE modifications at DSS 14.

335 First scheduled XBTE pass; cancelled because DSS 14 not ready to support.

338 Approval of ECO 75.312 - temporary X-band AGC and T_{op} recordings.

341 Second scheduled XBTE pass; cancelled by DSN because not enough pre-pass time for setup.

342 Third scheduled XBTE pass; DSS 14 personnel had trouble getting experiment going due to lack of familiarity - dry run would have been helpful; DSS 14 op's setup 60 KHz subcarrier instead of 240 KHz - couldn't lock SDA's as result; Doppler predicts furnished to op's were in error; one of bit error counters did not survive trip out to station; initial data rate of 24 Kbps too high for computer program for recording - needed slight program change; did get seven minutes of questionable X-band data.

344 Fourth scheduled pass; line driver for S-band clock went bad early in pass; had d.c. offset problems in amplifiers; op's had used wrong mod index setting on SDA's - changed this and signals improved; made recordings at S- and X-bands on and off for three hour period; this pass and the one on day 342 turned out to be the dry run.

345 Fifth scheduled pass; first really successful recording of both S- and X-data; delay in setup of SCA - new shift at DSS 14; another delay caused by problems in antenna pointing system;

after processing mag tape recordings, found that S-band ADC amplitude was set too high - thus grossly degrading SNORE - this led to the analysis in Appendix C; just prior to the pass rain squalls appeared in the Goldstone area - a sharp increase in system temperature was noted on the X-band radiometer at the Venus site and coincided with heavy rainfall at the site during that period; little rain fell at DSS 14 - none during the pass.

357 Sixth scheduled pass; change of shift near start of pass caused confusion and led to no calibration of X-band T_{op}; receiver 4 found to be functioning improperly; TCP β down; this meant no X-band SSA SNORE on station link printer; delay due to reconfiguring S- and X- strings of RCV, SDA, SSA; recordings successful on S- and X- for most of pass.

359 Seventh scheduled pass; this was Christmas Eve and XBTE experimenters did not go to DSS 14; however, had station personnel set up experiment with intention of getting T_{op} and AGC recordings as well as SSA SNORE on station line printer; unfortunately, RCV 4 (on α string) was still down as well as TCP β and thus could not get SNORE on X-band.

363 Eighth scheduled pass; XRO maser (X-band) down; tried 70 Kbps on S-band but operators couldn't lock SDA with data rates higher than 25-Kbps; subsequent tests in TDL indicate the SDA should have locked; recorded no data.

14 Ninth scheduled pass; CONSCAN computer down - servo manually controlled; successfully recorded S- and X- data.

16	Tenth scheduled pass; DIS down - no SNORE on line printer; S- and X- data successfully recorded.
17/18	Eleventh scheduled pass; DIS still down - no SNORE on line printer; X-data successfuly recorded; hardware failure on S-mag tape recording.

Table B1

Condensed Diary for Successful Passes

PARAMETERS	DATES 345	357	14	16	17/18
Spacecraft No.	2	1	2	1	1
Times of Data Taking (GMT)	0400-1200	0300-1100	0300-1100	0300-1100	2300-1100
X-band String:					
RCV	3	3	4	4	4
SDA	6	6	2	2	2
SSA	4	4	1	2	2
S-band String:					
RCV	1	1	3	3	3
SDA	2	2	5	5	5
SSA	2	2	4	4	4
Data Rates (Kbps):					
(1)	22	10	5	4	4
(2)	-	20	7	5	5
Time of data Rate Change (GMT)	-	0750	0525	0406	0630
Successful SNR Measurements:	S/X	S/X	S/X	S/X	S/X
Bit Error Counter	Yes/Yes	Yes/Yes	Yes/Yes	Yes/Yes	Yes/Yes
Mag Tape SNORE	No/Yes	Yes/Yes	Yes/Yes	Yes/Yes	No/Yes
SSA SNORE	Yes/Yes	Yes/No	Yes/Yes	No/No	No/No
Calculated SNR	Yes/Yes	Yes/No	Yes/Yes	No/No	Yes/Yes

APPENDIX C

Effect of ADC Amplitude Settings on SNORE

The setting of the amplitude of the integrate and dump samples prior to sampling by the analog to digital converter (ADC) is critical for SNORE calculations. As described in Appendix A, an 8-bit ADC was used for sampling the integrate and dump outputs from the SSA's. However, only the most significant bit (the sign bit) and the five least significant bits are used so that the ADC is effectively a 6-bit ADC. The problem arises from the fact that voltages beyond the range of the five least significant bits make use of the two unused bits. The effect is that these higher voltages get converted into numbers which are modulo-100000 (binary) in the positive case and similarly for negative voltages. This foldover phenomenon can cause severe degradation in calculating SNORE from the sample values. Thus, the amplitude cannot be set too large. On the other hand, if the voltage amplitudes are set too small, quantization error becomes a factor because the full range of the ADC is not being utilized. Thus, some optimum setting exists to get the least degradation in the SNORE calculation.

For purposes of analysis, the assumption is made that only 1's are transmitted as data. The voltage assignments for the ADC are as follows. Bin i refers to the ADC number generated by any voltage in the range

$$\frac{V_m}{2^{N-1}}(i - \tfrac{1}{2}) \leq V_i \leq \frac{V_m}{2^{N-1}}(i + \tfrac{1}{2}) \qquad \text{C.1}$$

where V_m is the maximum ADC voltage and N is the number of the used bits in the ADC (6 in this case). The voltage assignment of C.1 implies that zero volts occur in the middle of bin "0" and that V_m goes in the non-existent bin 2^{N-1}. (The highest positive bin is $2^{N-1} - 1$).

In order to calculate the mean and variance of the ADC numbers, it is necessary to know the probability that a sample will occupy bin i. Thus,

$$P_i \triangleq \text{Prob } \{\text{occurrence of sample } i\} \tag{C.2}$$

If one "foldover" in voltage is assumed for positive voltages, then

$$P_i \simeq \text{Prob } \{\text{sample voltage falls in bin } i\} + \text{Prob } \{\text{sample voltage falls in bin } i + 2^{N-1}\} \quad i \geq 0 \tag{C.3}$$

The assumption in C.3 is that because of the Gaussian distribution of the samples, it is unlikely that further foldovers would be significant. Now for the negative bins the assumption that all 1's are sent implies a positive mean. Therefore, a reasonable assumption is that a small percentage of foldovers occur for negative voltages, i.e.

$$P_i \simeq \text{Prob } \{\text{sample voltage falls in bin } i\} \quad i < 0 \tag{C.4}$$

Now for PSK, the integrate and dump output has a Gaussian distribution with mean A (volts) and variance of

$$\sigma^2 = \frac{N_0}{2T} \tag{C.5}$$

where N_0 is the one-sided noise spectral density (W/Hz) and T is the bit time. Using the assumptions of C.3 and C.4, P_i can be written as

$$P_i = \begin{cases} Q\left\{\left[\frac{V_m}{A}\left(\frac{i-\frac{1}{2}}{2^{N-1}}\right)-1\right]\sqrt{2\frac{ST}{N_o}}\right\} \\ \quad - Q\left\{\left[\frac{V_m}{A}\left(\frac{i+\frac{1}{2}}{2^{N-1}}\right)-1\right]\sqrt{2\frac{ST}{N_o}}\right\} & ; i<0 \\ \hline Q\left\{\left[\frac{V_m}{A}\left(\frac{i-\frac{1}{2}}{2^{N-1}}\right)-1\right]\sqrt{2\frac{ST}{N_o}}\right\} \\ \quad - Q\left\{\left[\frac{V_m}{A}\left(\frac{i+\frac{1}{2}}{2^{N-1}}\right)-1\right]\sqrt{2\frac{ST}{N_o}}\right\} \\ \quad + Q\left\{\left[\frac{V_m}{A}\left(\frac{i-\frac{1}{2}+2^{N-1}}{2^{N-1}}\right)-1\right]\sqrt{2\frac{ST}{N_o}}\right\} \\ \quad - Q\left\{\left[\frac{V_m}{A}\left(\frac{i+\frac{1}{2}+2^{N-1}}{2^{N-1}}\right)-1\right]\sqrt{2\frac{ST}{N_o}}\right\} & ; i \geq 0 \end{cases} \quad \text{C.6}$$

where

$$Q(x) = \frac{1}{\sqrt{2\pi}} \int_x^\infty e^{-t^2/2}\, dt \quad \text{C.7}$$

and

$$\frac{ST}{N_o} = \frac{A^2}{2\sigma^2} \quad \text{C.8}$$

This latter term, ST/N_o is the desired signal to noise ratio (SNR) which the SNORE algorithm estimates by the formula

$$SNR = \frac{(MEAN)^2}{2\ (VARIANCE)} \quad \text{C.9}$$

where

$$MEAN = \sum_{i=-2^{N-1}}^{2^{N-1}-1} i\, P_i \quad \text{C.10}$$

$$VARIANCE = \sum_{i=-2^{N-1}}^{2^{N-1}} i^2\, P_i - (MEAN)^2 \quad \text{C.11}$$

What is desired, therefore, is the difference between the true SNR (ST/N_o)

and that given by C.9 using C.6, etc. Clearly this difference is a function of A/V_m. That is, there exists an optimum setting of the signal mean voltage as a fraction of the maximum ADC voltage, V_m. This optimum setting is a function of the signal to noise ratio. This difference is plotted in Figure C1. for a variety of signal to noise ratios.

A couple of conclusions can be drawn from Figure C1. First of all, the voltage setting of the signal mean during the experiment is strictly an "eyeball" type adjustment. That is, the setting must be made with noisy signals so that an accurate setting is not possible. Because the degradation increases rapidly for A/V_m greater than the optimum setting, an attempt was always made to set the voltage slightly less than optimum. It should be emphasized, therefore, that some SNORE degradation is hard to avoid.

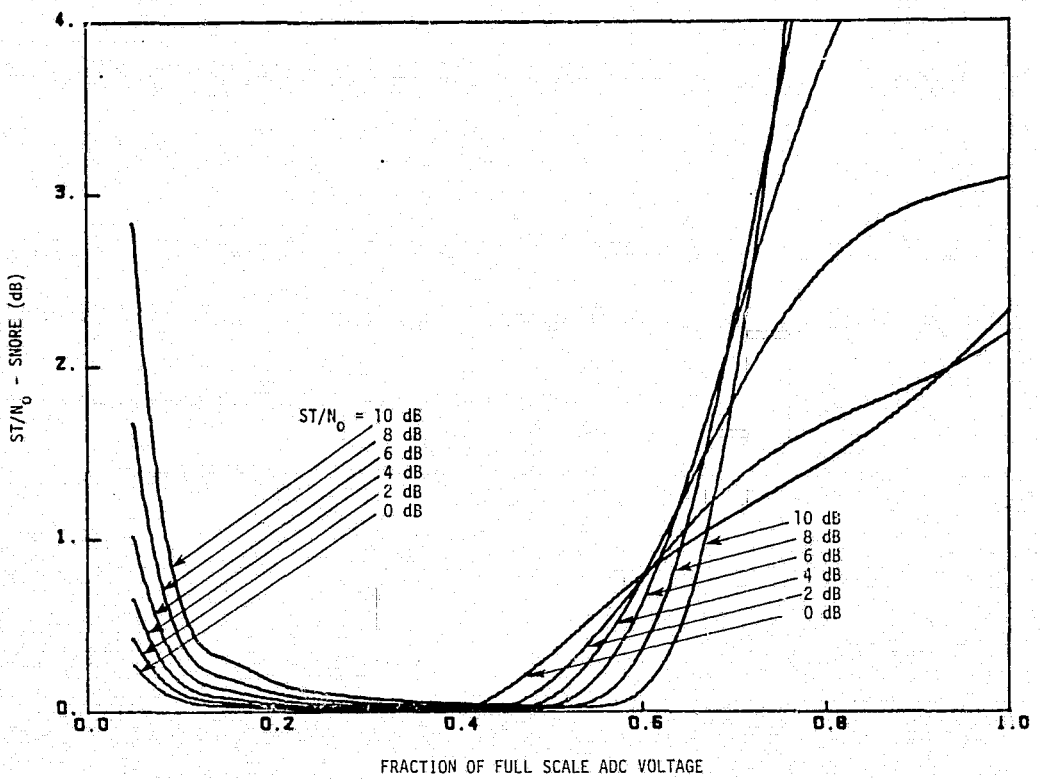

Fig. C1. SNORE degradation vs ADC input voltage

NASA—JPL—Coml, L A, Calif